THE JOURNAL OF PHYSICAL CHEMISTRY B

Article

pubs.acs.org/JPCB

Hydrogen Bonding versus $\pi-\pi$ Stacking Interactions in Imidazolium–Oxalatoborate Ionic Liquid

Yong-Lei Wang,*[,†] Aatto Laaksonen,[‡] and Michael D. Fayer[†]

[†]Department of Chemistry, Stanford University, Stanford, California 94305, United States

[‡]Department of Materials and Environmental Chemistry, Arrhenius Laboratory, Stockholm University, SE-106 91 Stockholm, Sweden

ABSTRACT: Intermolecular features like hydrogen bonding and π-type interactions play pivotal roles in stabilizing molecular structures in ionic liquids with planar rings and hydrogen-bond donors and acceptors. However, the delicate interplay among these interactions is complicated and depends on specific ion types. In this work, *ab initio* molecular dynamics simulations were performed to reveal competitive and cooperative characteristics among hydrogen bonding and π-type interactions in a typical imidazolium–oxalatoborate ionic liquid. Imidazolium rings take preferential on-top parallel orientations, leading to their particular $\pi-\pi$ stacking distributions at short distances. Intermolecular interactions between imidazolium and oxalato rings are manifested by short-range on-top parallel orientations and in-plane hydrogen bonding interactions, promoting their parallel displaced offset stacking arrangements. However, on an intermediate distance scale, attractive Coulombic interactions between imidazolium and oxalato rings dominate and contribute to their perpendicular orientations. Spatial coordination patterns between intermolecular oxalato rings are balanced by repulsive electrostatic interactions and steric hindrance effects, leading to their tilted orientations in local environments.

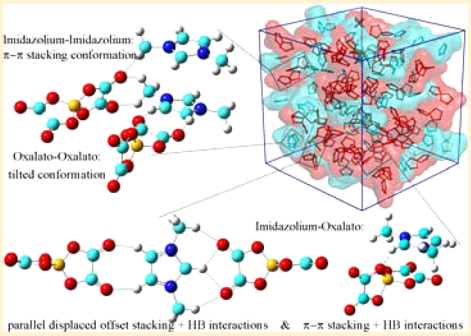

I. INTRODUCTION

Room-temperature ionic liquids (ILs) are a novel category of molten salts entirely composed of ionic species. The bulky and irregular shapes of ionic groups, often consisting of conformationally flexible hydrocarbon chains and ring structures, enhance entropy effects, and thus inhibit crystallization at room temperature in spite of strong Coulombic interactions.[1,2] By selecting proper anions and adjusting the hydrocarbon chain lengths of cations, ILs' physicochemical properties can be systematically tailored to meet specific requirements. These finely tunable properties render them outstanding green alternatives to corrosive, volatile, and polluting solvents,[3] useful reaction media and working fluids in the chemical industry,[4,5] valuable solvents for microlubrication and nanotribology,[6,7] and multiphasic separation.[8]

The intense academic and industrial interest in ILs stems from their complex combination of molecular level interactions. Strong Coulombic and favorable van der Waals interactions are key driving forces but can have opposite effects for ionic species. The trade-offs between these molecular interactions can give rise to strikingly shallow potential energy surfaces such that even weak contributions can result in significant differences in molecular structures and change ILs' functional performance in industrial applications.[2,4−6]

Delicate intermolecular interactions, like hydrogen bonding (HB) and π-type interactions that rarely occur simultaneously in traditional molten salts,[2,9] are critical for the formation of particular ionic structures in bulk and confined environments.[2,5−7] However, the nature of these interactions is distinctive and complex. HB is mainly determined by covalent, electrostatic, and charge-transfer interactions, and is a key driving force for local structuring in solid and liquid phases,[10−12] as well as affecting heterogeneous dynamics and the viscosity of ILs.[12−14] In contrast to HB, π-type interactions are related to electrostatic and dispersion interactions only[15,16] and play essential roles in molecular recognition among ionic species.[15,17−19]

For imidazolium cations coupled with small anions, such as Cl^-,[15,17,18] SCN^-,[17] and NO_3^- anions,[19] HB and π-type interactions simultaneously occur between ionic species. Their cooperative effect promotes the formation of prominent ordered microstructures in bulk ionic liquids. However, when imidazolium cations are associated with large anionic groups, like bis(trifluoromethylsulfonyl)imide (NTf_2^-),[13,20,21] both HB and π-type interactions are considerably weakened in the liquid phase of corresponding ILs. Large anions typically have multiple HB interaction sites within the liquid environment and exhibit reduced HB strength and directionality. Additionally, these large anions take preferential on-top distributions above and below imidazolium rings, leading to π-type interactions being partially or totally blocked due to anionic size effect. The delicate interplay of HB and π-type interactions among ionic species, either competitive or cooperative, becomes more complicated than this intuitive explanation implies if anions have ring structures, like the chelated

Received: June 6, 2017
Published: July 10, 2017

DOI: 10.1021/acs.jpcb.7b05564
J. Phys. Chem. B 2017, 121, 7173−7179

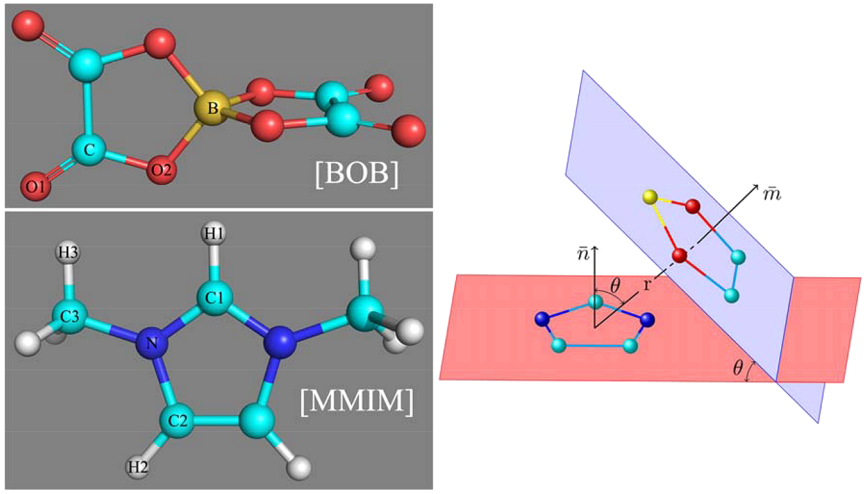

Figure 1. Molecular structures of the [MMIM] cation and the [BOB] anion with representative atom types and relative orientation of imidazolium-oxalato ring planes. Imidazolium and oxalato rings refer to those formed by C1-N-C2-C2-N atoms, and by B-O2-C-C-O2 atoms in consecutive orders, respectively. r is the radial distance between the center-of-mass of the imidazolium and the oxalato rings. $\bar{n}$ and $\bar{m}$ represent normal vectors to imidazolium and oxalato ring planes, respectively. θ is the angle between two normal vectors and also the angle between two ring planes.

orthoborate families.[22,23] These intermolecular interactions are quite sensitive to detailed electronic structures and the molecular geometries of anions in local environments, and their subtle balance will intrinsically determine ILs' physicochemical properties and subsequently, their industrial applications.

In this study, we provide physical insights into the complex interplay between HB characteristics and π-type stacking features in dimethylimidazolium bis(oxalato)borate ([MMIM][BOB]) ionic liquid through *ab initio* molecular dynamics (AIMD) simulations. This IL was selected because of the relative simplicity of the [MMIM] cation and the [BOB] anion, but essential intermolecular interactions, like HB, π-type stacking, and possible C−H···π and C═O···π interactions between [MMIM] cations and [BOB] anions are included. Typical molecular structures and representative atom types are shown in Figure 1.

II. SIMULATION METHODOLOGY

A. Classic Molecular Dynamics Simulations. Classic molecular dynamics simulations of [MMIM][BOB] ionic liquid were first performed using GROMACS 5.0.4 package[24] with three-dimensional periodic boundary conditions. The equations of motion were integrated using the leapfrog integration algorithm with a time step of 1.0 fs. A cutoff radius of 1.6 nm was set for short-range van der Waals interactions and real-space electrostatic interactions. The Particle-Mesh Ewald summation method with an interpolation order of 5 and Fourier grid spacing of 0.12 nm was employed to handle long-range electrostatic interactions in reciprocal space.

In the current atomistic simulations, an IL system consisting of 448 [MMIM][BOB] ion pairs was constructed. Atomistic force field parameters between ionic species were adopted from previous work[22] based on the AMBER framework. This IL system was first energetically minimized using a steepest descent algorithm and thereafter annealed gradually from 800 to 400 K within 10 ns. The annealed simulation box was equilibrated in an NPT (isothermal−isobaric) ensemble for at least 40 ns of physical time, maintained using the Nosé−Hoover chain thermostat and the Parrinello−Rahman barostat with time coupling constants of 500 and 200 fs, respectively, to control the temperature at 400 K and the pressure at 1 atm. The liquid density for [MMIM][BOB] is 1.5059 g/cm^3 at 400 K, which is quite close to the experimental value of 1.4837 g/cm^3 at the same temperature.[25] It should be noted that the melting point of [MMIM][BOB] IL is within 312−320 K depending on the content of residual impurities in the ionic liquid. This temperature range is a little higher than room temperature, so we choose an elevated temperature, i.e., 400 K, to simulate [MMIM][BOB] IL at its liquid state.

A representative configuration consisting of 56 [MMIM][BOB] ion pairs was taken from the above pre-equilibrated simulation box. This representative ionic structure was energetically minimized, annealed from 800 to 400 K within 5 ns, and equilibrated in an NVT ensemble for 20 ns at 400 K in a simulation box which has the same size as that for 448 [MMIM][BOB] ion pairs. Atomistic simulations in the NPT ensemble were then performed for another 20 ns at the same temperature to equilibrate the simulation system and to shrink the simulation box to proper size. Thereafter, the simulation box size was slightly adjusted leading to a cubic box with a cell vector of 2.5979 nm, which has the same density as that yielded from "large" simulation system consisting of 448 [MMIM][BOB] ion pairs. The final configuration consisting of 56 [MMIM][BOB] ion pairs from the above atomistic simulations was used as a starting point to set up AIMD simulations.

B. Ab Initio Molecular Dynamics Simulations. AIMD simulations were performed using the QUICKSTEP Module[26] implemented in the CP2K program and an orbital transformation approach[27] that utilizes hybrid Gaussian and plane wave basis sets to calculate energies and forces on atoms for faster convergence. The electronic structures were calculated employing density functional theory utilizing the BLYP exchange-correlation functional[28,29] with Grimme's empirical dispersion correction D3,[30] which has proven successful in the description of ionic liquid structures.[17,21,31] The molecularly optimized double-ζ basis set (MOLOPT-DZVP-SR-GTH)[32] with corresponding Goedecker−Teter−Hutter (GTH) pseudopotentials[33] were applied to all atom types. A 300 Ry density CUTOFF criterion for the finest grid level was employed in density functional theory calculations together with multigrid number 5 along with density smoothing for electron density

DOI: 10.1021/acs.jpcb.7b05564
J. Phys. Chem. B 2017, 121, 7173−7179

(NN10-SMOOTH) and its derivative (NN10). AIMD simulations were carried out using a time step of 0.4 fs and a SCF convergence criterion of 10^{-6} in an NVT ensemble at 400 K maintained using a Nosé−Hoover chain thermostat. The simulation box was first equilibrated for 12 ps and thereafter sampled for 48 ps with a time interval of 0.8 fs in dumping coordinates, forces, and velocities for all atoms.

The AIMD simulation was conducted at elevated temperature, i.e., at 400 K. This choice ensures that the [MMIM][BOB] IL is in its liquid state with a low viscosity and thus enhanced the sampling of different configurations in phase space without a significant change in electronic properties. This procedure is a popular way to study the microstructural and dynamical properties of ILs.[17,21,31] On the basis of previous temperature dependent studies,[34,35] we expect that the present AIMD simulations of [MMIM][BOB] IL will produce microstructural properties representative of the [MMIM][BOB] IL in its liquid phase.

III. RESULTS AND DISCUSSION

Figure 2 presents radial and combined distribution functions (CDFs) between centers-of-mass (COM) of imidazolium and oxalato rings. A relatively weak and one strong coordination regime, labeled as I and II, are shown in CDFs for imidazolium−imidazolium and imidazolium−oxalato pairs in Figure 2A,B, respectively. Weak coordination patterns are mainly registered in domains with the angle between ring planes of approximately 20° and with a COM radial distance of 0.4 nm, indicating the presence of π-type interactions between ring planes.[17,18] The weak association region for intermolecular oxalato−oxalato pairs shown in Figure 2C is seen near 0.45 nm and around 40°, suggesting that this is the most probable tilted orientation of oxalato rings to those in neighboring [BOB] anions. These implied π-type features and tilted orientations of ring structures are qualitatively reflected in broad shoulders and prepeaks at short distances in the corresponding radial distribution functions (RDFs). The strong coordination regimes in the CDFs for imidazolium−imidazolium, imidazolium−oxalato, and oxalato−oxalato pairs are registered in large angular distributions (50−90°) and different radial distances owing to the delicate compromise between strong and weak intermolecular interactions among ionic species. The large amplitude in the imidazolium−oxalato RDF curve and the distinctive coordination pattern in Figure 2B indicate highly ordered ionic structures among imidazolium and oxalato rings. Imidazolium rings are preferentially localized around neighboring [BOB] anions and exhibit tilted and favorable perpendicular orientations to oxalato ring planes. Such an ionic structure mainly originates from strong attractive electrostatic interactions between imidazolium and oxalato rings. The intermediate coordination patterns in imidazolium−imidazolium and oxalato−oxalato CDFs are characterized with perpendicular features at large radial distances due to electrostatically repulsive interactions between ionic species carrying the same charges. However, such perpendicular orientations are relatively weak compared with those for imidazolium−oxalato pairs, possibly owing to anionic steric hindrance.

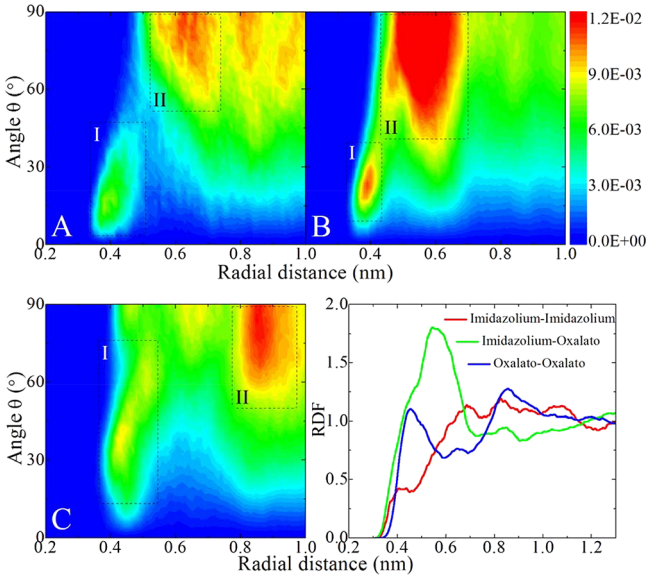

Figure 2. Radial and combined distribution functions among the COMs of imidazolium and oxalato rings. Panels (A), (B), and (C) present θ angles for imidazolium−imidazolium, imidazolium−oxalato, and oxalato−oxalato pairs vs the corresponding radial distances between COMs of ring planes, respectively.

Given that π-type interactions can be classified into parallel and parallel displaced offset stacking orientations,[18] we further clarify detailed interaction types in three CDFs through spatial distribution functions (SDFs)[36] shown in Figure 3. In the SDF contour surfaces for imidazolium−imidazolium presented in Figure 3A, the solid-green contours above and below the imidazolium ring correspond to the prepeak in the corresponding RDF curve and the weak coordination pattern in the CDF plot. These two contours are located within the first solvation shell of a central imidazolium ring plane with the distance to the COM of the imidazolium plane being less than 0.46 nm, demonstrating a strict parallel $\pi-\pi$ stacking feature of neighboring imidazolium rings.[15,17] Typical imidazolium−imidazolium ionic structures are provided in Figure 4A. Further structural analysis shows that there are approximately 15% of close-contact imidazolium rings taking on $\pi-\pi$ stacking conformations, and the other 85% of imidazolium ring pairs exhibiting either tilted configurations along ring−methyl vectors or other conformations at larger distances.

The COMs of imidazolium rings around neighboring [BOB] anions, as shown in Figure 3B, are characterized by broad distributions. The most probable density contours are localized near oxygen atoms (both O1 and O2 atoms as labeled in Figure 1) and above and below oxalato ring planes of the [BOB] anion. It should be noted that it is difficult to visualize the individual contributions of the weak coordination pattern in this SDF plot as (i) this weak contribution is buried in the equatorial region of oxalato ring plane, and (ii) this coordination pattern is far weaker than the decisive counterpart shown at a large radial distance in Figure 2B, which is induced by strong attractive electrostatic interactions between the imidazolium and oxalato rings. However, the SDF contours of the COMs of oxalato rings around the [MMIM] cation present distinct short-range spatial distributions along the C1−H1 and C2−H2 vectors, and above/below the imidazolium ring plane as presented in Figure 3C. The former indicates that oxalato rings take parallel displaced offset stacking conformations around imidazolium rings, possibly promoting HB interactions between imidazolium and oxalato rings, as shown in typical imidazolium-oxalato ionic structures in Figure 4C. The latter corresponds to the essential $\pi-\pi$ stacking distributions between

DOI: 10.1021/acs.jpcb.7b05564
J. Phys. Chem. B 2017, 121, 7173−7179

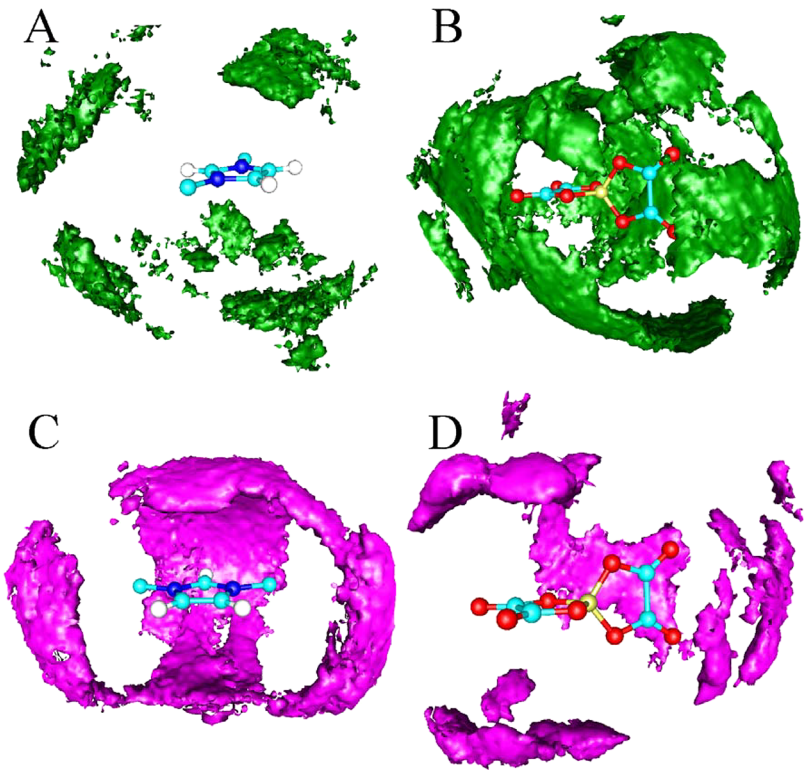

Figure 3. Three-dimensional density distribution functions of the COMs of imidazolium rings around [MMIM] (A) and [BOB] (B) and of the COMs of oxalato rings around [MMIM] (C) and [BOB] (D), respectively. The solid contours correspond to 3× the atom number densities relative to the corresponding average densities in the bulk region.

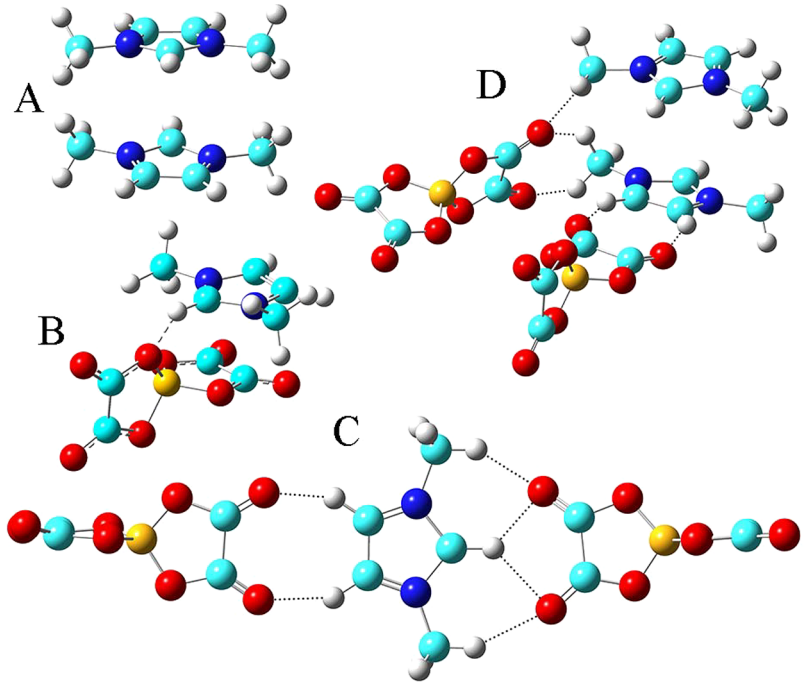

Figure 4. Representative molecular distributions and orientations among close-contact ionic groups. (A) Imidazolium−imidazolium pair featured with $\pi-\pi$ stacking orientation. The imidazolium−oxalato pair characterized by $\pi-\pi$ stacking (B) and parallel displaced offset stacking conformations (C) as well as HB interactions between hydrogen atoms in [MMIM] cations and oxygen atoms in [BOB] anions. (D) Oxalato−oxalato pair described by tilted molecular distributions that promote HB interactions with neighboring [MMIM] cations.

close-contact imidazolium and oxalato ring planes at short distance, and a representative ionic structure is shown in Figure 4B. AIMD simulation results indicate that for all close contact imidazolium-oxalato pairs with their COM distances being less than 0.43 nm, 42% of them exhibit parallel displaced offset stacking conformations, 31% present essential parallel orientations, and the remaining 27% show tilted distributions in the transition regions in SDF contours, respectively. The magenta

DOI: 10.1021/acs.jpcb.7b05564
J. Phys. Chem. B 2017, 121, 7173−7179

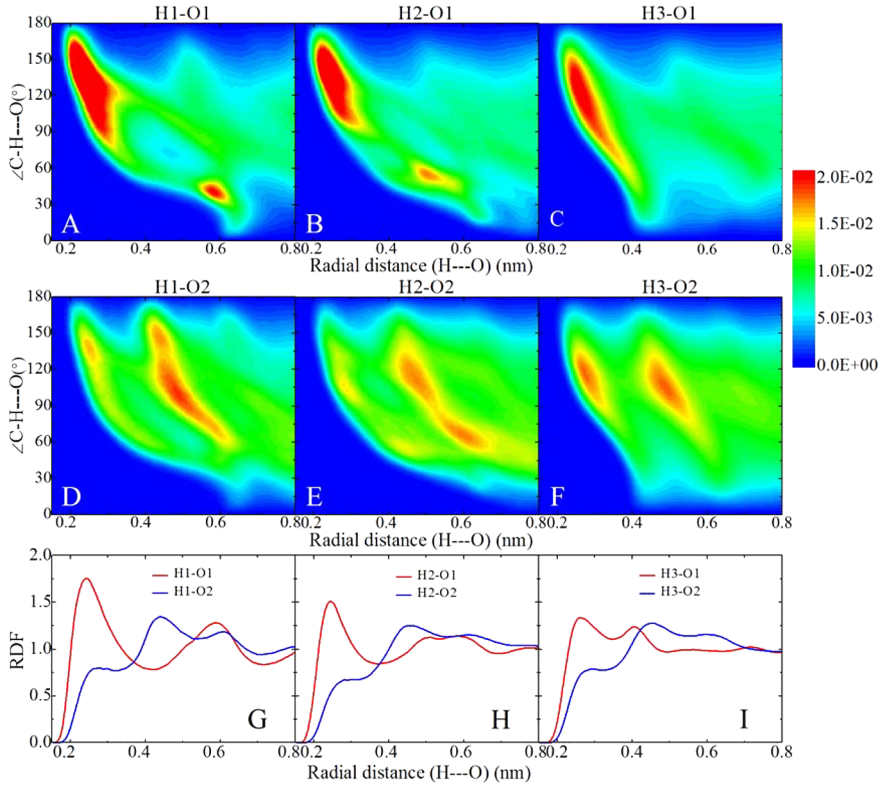

Figure 5. Combined distribution functions of ∠C−H···O vs $r_{H\cdots O}$ for three hydrogen types in [MMIM] cation and two oxygen types in [BOB] anion and corresponding radial distribution functions between respective hydrogen and oxygen atoms in ionic species.

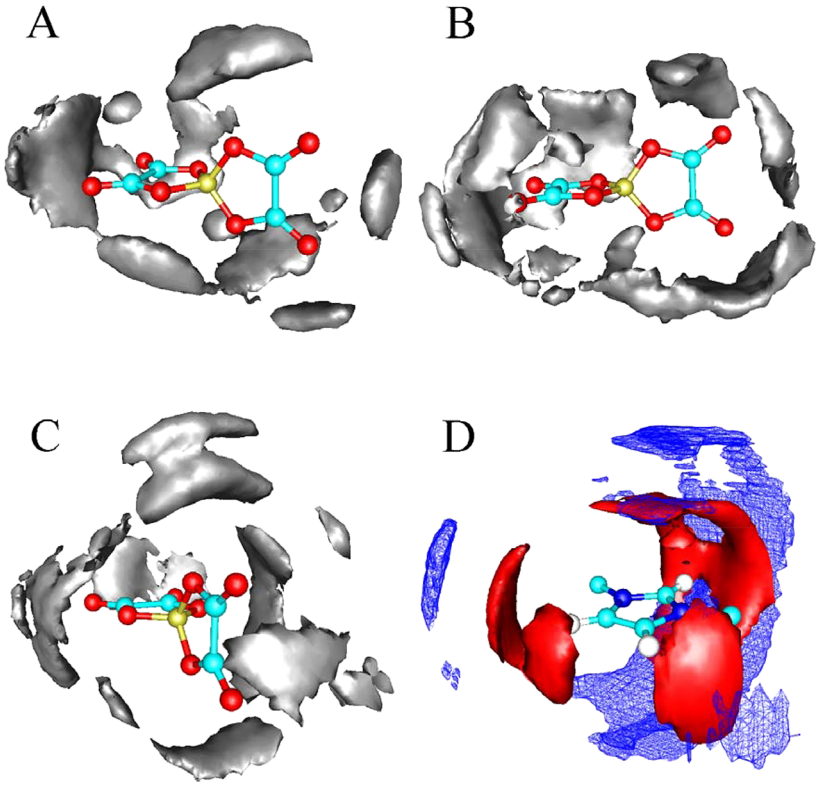

Figure 6. Three-dimensional distribution functions of (A) H1, (B) H2, (C) H3 atoms around a central [BOB] anion and of (D) O1 (solid red) and O2 (meshed blue) atoms around a central [MMIM] cation, respectively. These solid and meshed contour surfaces correspond to local high (3×) and low (2×) atom number densities relative to corresponding average density values in the bulk region, respectively.

contour surfaces in Figure 3D suggest that COMs of intermolecular oxalato rings are generally positioned above and below oxalato planes in neighboring [BOB] anions within 0.6 nm and take tilted conformations with approximately 45°

DOI: 10.1021/acs.jpcb.7b05564
J. Phys. Chem. B 2017, 121, 7173−7179

angles between close-contact oxalato ring planes. Representative intermolecular structures between close contact [BOB] anions are displayed in Figure 4D.

In ILs bearing imidazolium cations, it is generally believed that the H1 atom (as labeled in Figure 1) is the main hydrogen bond donating site, and HB interactions are mainly localized along the C1−H1 vector beyond the imidazolium ring. However, it was shown in experimental characterizations[13,37] and first-principles calculations[15,18,19] that both the H2 and H3 atoms contribute to considerable HB characteristics depending on the specific nature of the anionic species. Figure 5 presents the CDFs of ∠C−H···O vs $r_{H\cdots O}$ for hydrogen atoms in the [MMIM] cation and for oxygen atoms in the [BOB] anion as well as the corresponding site−site RDFs. All three hydrogen types exhibit distinctive and preferential HB interactions with O1 atoms, and the corresponding HB characteristics follow an order of H1 > H2 > H3. In the meantime, these hydrogen atoms also exhibit considerable HB coordination with O2 atoms in [BOB] anions with comparable strength. It is noteworthy that the HB features of these three hydrogen atoms to O2 atoms are much weaker than their counterparts to O1 atoms, as quantitatively manifested in respective CDF plots and RDF curves.

The particular HB coordination patterns are visualized in three-dimensional distribution functions of hydrogen atoms in the [MMIM] cation around a central [BOB] anion, and of O1/O2 atoms in the [BOB] anion around a central [MMIM] cation, respectively, as shown in Figure 6. All of the hydrogen atoms are mainly positioned around O1 atoms in the equatorial regions of oxalato rings, contributing to directional HB interactions between hydrogen atoms and O1 atoms in neighboring [BOB] anions and the formation of parallel displaced offset stacking conformations in close contact imidazolium-oxalato ring pairs (Figure 4C). In addition, these hydrogen atoms are also distributed around the central tetrahedron domain in coordinating O2 atoms in [BOB] anions. The HB coordination between hydrogen and O2 atoms is less favorable and can be considered as a secondary HB interaction between [MMIM] and [BOB] ions, which contributes to the stabilization of the $\pi-\pi$ stacking conformation between the imidazolium and oxalato ring planes (Figure 4B). The primary HB coordination of hydrogen atoms to O1 atoms and the formation of secondary hydrogen bonds between these hydrogen atoms and O2 atoms tend to flatten the potential energy surface between [MMIM] and [BOB] ionic groups. The flattened potential energy surface makes [MMIM][BOB] IL more fluid in contrast to imidazolium cations coupled with small anions having high interaction energies.[15,17−19]

It is significant to verify that both O1 and O2 atoms present particular spatial distributions around a central [MMIM] cation. The O1 atoms (solid-red contours in Figure 6D) are essentially localized along ring C−H vectors and above/below imidazolium ring plane, contributing to directional HB interactions as reflected in the strong coordination patterns shown in the top panels in Figure 5. The meshed-blue contours in Figure 6D correspond to the second coordination shell ($0.4 < r_{H\cdots O} < 0.6$ nm) between hydrogen atoms and O2 atoms shown in the middle panels in Figure 5, in which the first coordination pattern overlaps with and is much weaker than that for the H−O1 pair and thus is not visible. Additionally, it is interesting to observe that there are two holes, both in solid-red and in meshed-blue contours for O1 and O2 atoms, respectively, around the C1−H1 region. The angle between the normal vector of the geometrical center of the two holes and the C1−H1 vector is approximately 20°. Such a spatial pattern is in contrast to the proposed Z-bond between the Cl^- anion and the C1−H1 vector from first-principles calculations on [MMIM]Cl.[38] This structural discrepancy mainly attests to the distinctive ionic structures of [BOB] anions and their packing restrictions around [MMIM] cations in IL matrix.

In the [MMIM][BOB] IL, it is expected that C−H···π and C═O···π interactions exist and compete with HB and π-type interactions between ionic species so as to (de)stabilize ionic structures in the liquid phase. However, our systematic CDF characterizations indicate that neither type of interaction is available. The AIMD simulation results show that both C−H and C═O vectors take general orientations relative to neighboring ring planes because the proposed C−H···π and C═O···π geometries have negligible electrostatic energy contributions in comparison with HB, $\pi-\pi$ stacking, and parallel displaced offset stacking interactions.

IV. CONCLUDING REMARKS

We have performed *ab initio* molecular dynamics simulations to explore competitive and cooperative effects of HB and π-type interactions between [MMIM] cations and [BOB] anions in the ionic liquid phase. Interactions between [MMIM] cations are stabilized by distinctive parallel $\pi-\pi$ stacking interactions between imidazolium rings at short distance. The parallel $\pi-\pi$ stacking interactions overtake repulsive electrostatic interactions and other weak intermolecular interactions in determining the relative distribution of imidazolium ring structures. The spatial orientations of imidazolium to neighboring oxalato rings are characterized by $\pi-\pi$ stacking and parallel displaced offset stacking conformations at short distances, and by sharp perpendicular distributions at intermediate distances, respectively. The former is stabilized by directional HB interactions between hydrogen atoms of [MMIM] cations and oxygen atoms of [BOB] anions, while the latter is dominated by attractive Coulombic interactions between ionic species. The coordination pattern between intermolecular oxalato rings in [BOB] anions is balanced by repulsive Coulombic interactions and steric hindrance effects, leading to their tilted orientation in coordinating neighboring imidazolium cations in the local ionic environment.

AUTHOR INFORMATION

Corresponding Author

*E-mail: wangyonl@gmail.com; Phone: 650-785-3771.

ORCID

Yong-Lei Wang: 0000-0003-3393-7257

Michael D. Fayer: 0000-0002-0021-1815

Notes

The authors declare no competing financial interest.

ACKNOWLEDGMENTS

We thank Professor Thomas E. Markland for helpful discussion and suggestion. Y.-L.W. gratefully acknowledges financial support from the Knut and Alice Wallenberg Foundation (KAW 2015.0417). A.L. acknowledges the Swedish Science Council for financial support. M.D.F. thanks the Division of Chemistry, Directorate of Mathematical and Physical Sciences, National Science Foundation (NSF) (CHE-1461477) for support. All of the AIMD simulations were performed using

DOI: 10.1021/acs.jpcb.7b05564
J. Phys. Chem. B 2017, 121, 7173−7179

computational resources provided by the Swedish National Infrastructure for Computing (SNIC) at PDC and NSC.

REFERENCES

(1) Pádua, A. A.; Costa Gomes, M. F.; Canongia Lopes, J. N. Molecular Solutes in Ionic Liquids: A Structural Perspective. *Acc. Chem. Res.* **2007**, *40*, 1087.
(2) Hayes, R.; Warr, G. G.; Atkin, R. Structure and Nanostructure in Ionic Liquids. *Chem. Rev.* **2015**, *115*, 6357.
(3) Rogers, R. D.; Seddon, K. R. Ionic Liquids–Solvents of the Future? *Science* **2003**, *302*, 792.
(4) Plechkova, N. V.; Seddon, K. R. Applications of Ionic Liquids in the Chemical Industry. *Chem. Soc. Rev.* **2008**, *37*, 123.
(5) Armand, M.; Endres, F.; MacFarlane, D. R.; Ohno, H.; Scrosati, B. Ionic-Liquid Materials for the Electrochemical Challenges of the Future. *Nat. Mater.* **2009**, *8*, 621.
(6) Zhou, F.; Liang, Y.; Liu, W. Ionic Liquid Lubricants: Designed Chemistry for Engineering Applications. *Chem. Soc. Rev.* **2009**, *38*, 2590.
(7) Perkin, S. Ionic Liquids in Confined Geometries. *Phys. Chem. Chem. Phys.* **2012**, *14*, 5052.
(8) Han, X.; Armstrong, D. W. Ionic Liquids in Separations. *Acc. Chem. Res.* **2007**, *40*, 1079.
(9) Weingärtner, H. Understanding Ionic Liquids at the Molecular Level: Facts, Problems, and Controversies. *Angew. Chem., Int. Ed.* **2008**, *47*, 654.
(10) Skarmoutsos, I.; Welton, T.; Hunt, P. A. The Importance of Timescale for Hydrogen Bonding in Imidazolium Chloride Ionic Liquids. *Phys. Chem. Chem. Phys.* **2014**, *16*, 3675.
(11) Hunt, P. A.; Ashworth, C. R.; Matthews, R. P. Hydrogen Bonding in Ionic Liquids. *Chem. Soc. Rev.* **2015**, *44*, 1257.
(12) Hunt, P. A. Why Does a Reduction in Hydrogen Bonding Lead to an Increase in Viscosity for the 1-butyl-2,3-dimethyl-imidazolium-based Ionic Liquids? *J. Phys. Chem. B* **2007**, *111*, 4844.
(13) Fumino, K.; Wulf, A.; Ludwig, R. Strong, Localized, and Directional Hydrogen Bonds Fluidize Ionic Liquids. *Angew. Chem., Int. Ed.* **2008**, *47*, 8731.
(14) Zahn, S.; Bruns, G.; Thar, J.; Kirchner, B. What Keeps Ionic Liquids in Flow? *Phys. Chem. Chem. Phys.* **2008**, *10*, 6921.
(15) Matthews, R. P.; Welton, T.; Hunt, P. A. Hydrogen Bonding and π-π Interactions in Imidazolium-Chloride Ionic Liquid Clusters. *Phys. Chem. Chem. Phys.* **2015**, *17*, 14437.
(16) Petkovic, M.; Ristic, M.; Etinski, M. Stability and Anharmonic N-H Stretching Frequencies of 1-Methylthymine Dimers: Hydrogen Bonding versus π-Stacking. *J. Phys. Chem. A* **2016**, *120*, 1536.
(17) Brüssel, M.; Brehm, M.; Pensado, A. S.; Malberg, F.; Ramzan, M.; Stark, A.; Kirchner, B. On the Ideality of Binary Mixtures of Ionic Liquids. *Phys. Chem. Chem. Phys.* **2012**, *14*, 13204.
(18) Matthews, R. P.; Welton, T.; Hunt, P. A. Competitive π Interactions and Hydrogen Bonding Within Imidazolium Ionic Liquids. *Phys. Chem. Chem. Phys.* **2014**, *16*, 3238.
(19) Matthews, R. P.; Ashworth, C.; Welton, T.; Hunt, P. A. The Impact of Anion Electronic Structure: Similarities and Differences in Imidazolium Based Ionic Liquids. *J. Phys.: Condens. Matter* **2014**, *26*, 284112.
(20) Deetlefs, M.; Hardacre, C.; Nieuwenhuyzen, M.; Padua, A. A.; Sheppard, O.; Soper, A. K. Liquid Structure of the Ionic Liquid 1, 3-Dimethylimidazolium Bis{(trifluoromethyl)-sulfonyl}-amide. *J. Phys. Chem. B* **2006**, *110*, 12055.
(21) Weber, H.; Hollóczki, O.; Pensado, A. S.; Kirchner, B. Side Chain Fluorination and Anion Effect on the Structure of 1-butyl-3-methylimidazolium Ionic Liquids. *J. Chem. Phys.* **2013**, *139*, 084502.
(22) Wang, Y.-L.; Shah, F. U.; Glavatskih, S.; Antzutkin, O. N.; Laaksonen, A. Atomistic Insight into Orthoborate-Based Ionic Liquids: Force Field Development and Evaluation. *J. Phys. Chem. B* **2014**, *118*, 8711.
(23) Wang, Y.-L.; Sarman, S.; Kloo, L.; Antzutkin, O. N.; Glavatskih, S.; Laaksonen, A. Solvation Structures of Water in Trihexyltetradecyl-phosphonium-Orthoborate Ionic Liquids. *J. Chem. Phys.* **2016**, *145*, 064507.
(24) Hess, B.; Kutzner, C.; Van Der Spoel, D.; Lindahl, E. GROMACS 4: Algorithms for Highly Efficient, Load-balanced, and Scalable Molecular Simulation. *J. Chem. Theory Comput.* **2008**, *4*, 435.
(25) Shimpi, M. R., Private Communication.
(26) VandeVondele, J.; Krack, M.; Mohamed, F.; Parrinello, M.; Chassaing, T.; Hutter, J. Quickstep: Fast and Accurate Density Functional Calculations Using a Mixed Gaussian and Plane Waves Approach. *Comput. Phys. Commun.* **2005**, *167*, 103.
(27) VandeVondele, J.; Hutter, J. An Efficient Orbital Transformation Method for Electronic Structure Calculations. *J. Chem. Phys.* **2003**, *118*, 4365.
(28) Becke, A. D. Density-Functional Exchange-Energy Approximation with Correct Asymptotic Behavior. *Phys. Rev. A: At., Mol., Opt. Phys.* **1988**, *38*, 3098.
(29) Lee, C.; Yang, W.; Parr, R. G. Development of the Colle-Salvetti Correlation-Energy Formula into a Functional of the Electron Density. *Phys. Rev. B: Condens. Matter Mater. Phys.* **1988**, *37*, 785.
(30) Grimme, S.; Antony, J.; Ehrlich, S.; Krieg, H. A Consistent and Accurate *ab initio* Parametrization of Density Functional Dispersion Correction (DFT-D) for the 94 Elements H-Pu. *J. Chem. Phys.* **2010**, *132*, 154104.
(31) Weber, H.; Kirchner, B. Complex Structural and Dynamical Interplay of Cyano-based Ionic Liquids. *J. Phys. Chem. B* **2016**, *120*, 2471.
(32) VandeVondele, J.; Hutter, J. Gaussian Basis Sets for Accurate Calculations on Molecular Systems in Gas and Condensed Phases. *J. Chem. Phys.* **2007**, *127*, 114105.
(33) Goedecker, S.; Teter, M.; Hutter, J. Separable Dual-Space Gaussian Pseudopotentials. *Phys. Rev. B: Condens. Matter Mater. Phys.* **1996**, *54*, 1703.
(34) Brüssel, M.; Brehm, M.; Voigt, T.; Kirchner, B. Ab Initio Molecular Dynamics Simulations of a Binary System of Ionic Liquids. *Phys. Chem. Chem. Phys.* **2011**, *13*, 13617.
(35) Wendler, K.; Dommert, F.; Zhao, Y. Y.; Berger, R.; Holm, C.; Delle Site, L. Ionic Liquids Studied Across Different Scales: A Computational Perspective. *Faraday Discuss.* **2012**, *154*, 111.
(36) Kusalik, P. G.; Svishchev, I. M. The Spatial Structure in Liquid Water. *Science* **1994**, *265*, 1219.
(37) Peppel, T.; Roth, C.; Fumino, K.; Paschek, D.; Köckerling, M.; Ludwig, R. The Influence of Hydrogen-Bond Defects on the Properties of Ionic Liquids. *Angew. Chem., Int. Ed.* **2011**, *50*, 6661.
(38) Dong, K.; Zhang, S.; Wang, Q. A New Class of Ion-Ion Interaction: Z-bond. *Sci. China: Chem.* **2015**, *58*, 495.

DOI: 10.1021/acs.jpcb.7b05564
J. Phys. Chem. B 2017, 121, 7173−7179